

Bis(iminoethyl)pyridine Systems with a Pendant Alkenyl Group. Part A: Cobalt and Iron Complexes and Their Catalytic Behavior[†]

Carolin Wallenhorst, Gerald Kehr, Heinrich Luftmann,[§] Roland Fröhlich,[‡] and Gerhard Erker*

Organisch-Chemisches Institut der Universität Münster, Corrensstrasse 40, 48149 Münster, Germany

Received July 30, 2008

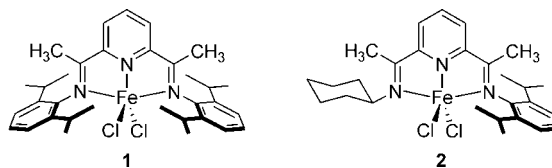
The acid-catalyzed reaction of 2,6-diacetylpyridine with 2,6-diisopropylaniline yielded the monoiminoethylpyridine derivative **3**. Its condensation reactions with allylamine or ω -aminobutene, -pentene, and -hexene furnished the unsymmetrically substituted 6-(*N*-(*n*-alkenyl)iminoethyl)-2-(*N*-(2,6-diisopropylphenyl)iminoethyl)pyridines **5a–d** (**5a–c** were characterized by X-ray diffraction). Treatment of the chelate ligands **5a–d** with CoCl₂ or FeCl₂ gave the respective cobalt (**7a–d**) and iron complexes (**8a–d**) in good yields (all cobalt complexes and **8b,c** were characterized by X-ray crystal structure analyses). The reaction of the cobalt(II) complex **7a** with 3 molar equiv of methyl lithium gave the corresponding tridentate chelate ligand Co(I) methyl complex **11a** (also characterized by X-ray diffraction). The complexes **7a–d**, **8a–d**, and **11a** were activated with methylalumoxane (Al:M = 300). The resulting cobalt-complex-derived homogeneous Ziegler–Natta catalysts produced polyethylene, albeit with a rather low activity. The iron-complex-derived catalysts were more active and gave mixtures of linear polyethylene and low-molecular-weight oligoethylenes.

Introduction

The advent of homogeneous Ziegler–Natta catalysts has brought substantial progress into the field of catalytic olefin polymerization. Subsequent to the group 4 metallocenes and related complexes¹ the late-transition-metal “post-metallocene” catalysts have received increased attention.² Among them the 2,6-bis(iminoalkyl)pyridine ligands were found to be especially useful. Their iron (and to a lesser extent cobalt) complexes often gave very active olefin polymerization catalysts when activated with methylalumoxane (MAO).³ The nature of the groups attached at the imino nitrogen atoms was found to be critical. Bulky 2,6-disubstituted aryl groups (e.g., 2,6-diisopropylphenyl as in **1**, which were oriented normal to the central ligand plane

and showed substantially hindered rotation around the N–C(aryl) vector) gave rise to very active catalyst systems for the production of linear, relatively high molecular weight polyethylene.³ Introduction of smaller substituents at the aryl groups led to ethylene oligomerization catalysts.⁴ Bianchini et al.^{5,6} have described unsymmetrical systems (such as **2**, see Scheme 1) where one of the bulky 2,6-diisopropylphenyl groups was replaced by an alkyl or aryl substituent. The catalysts derived from such Fe complexes still were very active but typically gave ethylene oligomers (in the C₁₀ to C₂₀ range) instead of polyethylene.⁵

Scheme 1



* To whom correspondence should be addressed. E-mail: erker@uni-muenster.de.

[†] Dedicated to Professor Helmut Schwarz on the occasion of his 65th birthday.

[‡] X-ray crystal structure analyses.

[§] Mass spectrometry.

(1) (a) Jordan, R. F. *Adv. Organomet. Chem.* **1991**, *32*, 325–387. (b) Brintzinger, H. H.; Fischer, D.; Mühlaupt, R.; Rieger, B.; Waymouth, R. M. *Angew. Chem.* **1995**, *107*, 1255–1283; *Angew. Chem., Int. Ed.* **1995**, *34*, 1143–1170. (c) McKnight, A. L.; Waymouth, R. M. *Chem. Rev.* **1998**, *98*, 2587–2598. (d) Okuda, J.; Eberle, T. Half-Sandwich Complexes as Metallocene Analogues In *Metallocenes-Synthesis, Reactivity, Applications*; Togni, A., Haltermann, R. L., Eds.; Wiley-VCH: Weinheim, Germany, 1998; Vol. 1, pp 415–453. (e) Chen, E. Y.-X.; Marks, T. J. *Chem. Rev.* **2000**, *100*, 1391–1434. (f) Erker, G. *Chem. Commun.* **2003**, 1469–147. (g) Erker, G.; Kehr, G.; Fröhlich, R. *J. Organomet. Chem.* **2004**, *689*, 4305–4318.

(2) (a) Britovsek, G. J. P.; Gibson, V. C.; Wass, D. F. *Angew. Chem.* **1999**, *111*, 448–468; *Angew. Chem., Int. Ed.* **1999**, *38*, 3842–8447. (b) Ittel, S. D.; Johnson, L. K.; Brookhart, M. *Chem. Rev.* **2000**, *100*, 1169–1203. (c) Gibson, V. C.; Spitzmesser, S. K. *Chem. Rev.* **2003**, *103*, 283–315. (d) Gibson, V. C.; Redshaw, C.; Solan, G. A. *Chem. Rev.* **2007**, *107*, 1745–1776.

(3) (a) Britovsek, G. J. P.; Gibson, V. C.; Kimberley, B. S.; Maddox, P. J.; McTavish, S. J.; Solan, G. A.; White, A. J. P.; Williams, D. J. *Chem. Commun.* **1998**, 849–851. (b) Small, B. L.; Brookhart, M.; Bennett, A. M. A. *J. Am. Chem. Soc.* **1998**, *120*, 4049–4050. (c) Margl, P.; Deng, L.; Ziegler, T. *Organometallics* **1999**, *18*, 5701–5708. (d) Deng, L.; Margl, P.; Ziegler, T. *J. Am. Chem. Soc.* **1999**, *121*, 6479–6487.

(4) Small, B. L.; Brookhart, M. *J. Am. Chem. Soc.* **1998**, *120*, 7143–7144.

(5) Bianchini, C.; Mantovani, G.; Meli, A.; Migliacci, F.; Zanobini, F.; Laschi, F.; Sommazzi, A. *Eur. J. Inorg. Chem.* **2003**, 1620–1631.

(6) (a) Small, B. L. *Organometallics* **2003**, *22*, 3178–3183. (b) Small, B. L.; Carney, M. J.; Holman, D. M.; O'Rourke, C. E.; Halfen, J. A. *Macromolecules* **2004**, *37*, 4375–4386. (c) Pelascini, F.; Wesolek, M.; Peruch, F.; Lutz, P. *J. Eur. J. Inorg. Chem.* **2006**, 4309–4316. (d) Bianchini, C.; Gatteschi, D.; Giambastiani, G.; Rios, I. G.; Ienco, A.; Laschi, F.; Mealli, C.; Meli, A.; Sorace, L.; Toti, A.; Vizza, F. *Organometallics* **2007**, *26*, 726–739. (e) Hao, P.; Zhang, S.; Sun, W.-H.; Shi, Q.; Adewuyi, S.; Lu, X.; Li, P. *Organometallics* **2007**, *26*, 2439–2446. (f) Sun, W.-H.; Hao, P.; Zhang, S.; Shi, Q.; Zuo, W.; Tang, X.; Lu, X. *Organometallics* **2007**, *26*, 2720–2734. (g) Barbaro, P.; Bianchini, C.; Giambastiani, G.; Rios, I. G.; Meli, A.; Oberhauser, W.; Segarra, A. M.; Sorace, L.; Toti, A. *Organometallics* **2007**, *26*, 4639–4651. (h) Bianchini, C.; Giambastiani, G.; Rios, I. G.; Meli, A.; Oberhauser, W.; Sorace, L.; Toti, A. *Organometallics* **2007**, *26*, 5066–5078. Review: (i) Bianchini, C.; Giambastiani, G.; Rios, I. G.; Mantovani, G.; Meli, A.; Segarra, A. M. *Coord. Chem. Rev.* **2006**, *250*, 1391–1418.

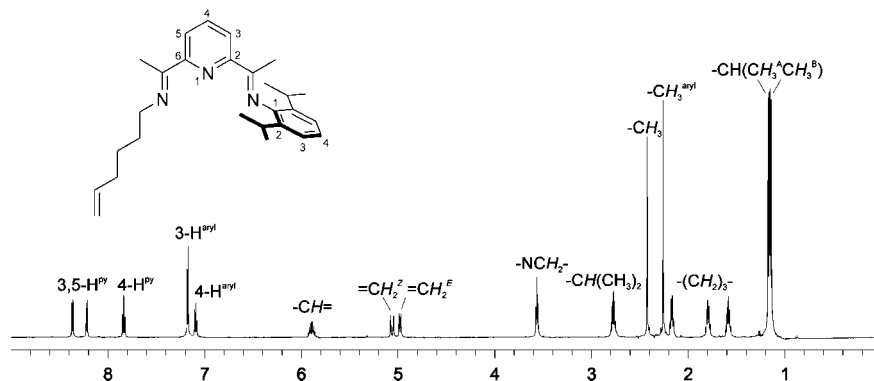


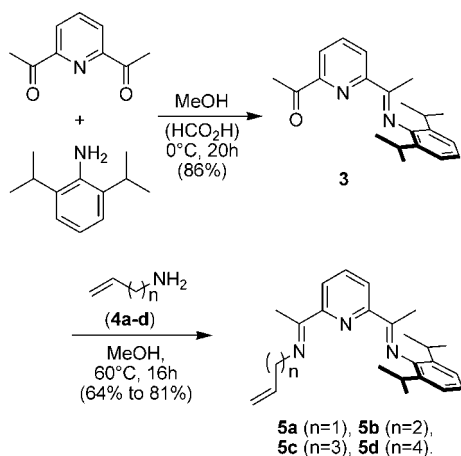
Figure 1. ^1H NMR spectrum (D_2 -dichloromethane, 600 MHz, 298K) of the hexenyl-substituted chelate ligand **5d**; aryl = 2,6-diisopropylphenyl.

We have now prepared a series of similar bis(iminoethyl)pyridine ligands bearing terminal alkenyl groups at one nitrogen and the usual 2,6-diisopropylphenyl substituent at the other. We synthesized their cobalt and iron complexes and found that some of the catalysts derived thereof showed some unexpected properties.

Results and Discussion

Synthesis and Characterization of the Ligands. The stepwise synthesis of the ligand systems **5a–d** is straightforward. The first condensation reaction to yield the monoimine system **3** was carried out by treatment of 2,6-diacetylpyridine with 2,6-diisopropylaniline in methanol at 0 °C with the aid of a small amount of formic acid as catalyst, analogous to the method described by Bianchini et al.^{5,7} A slight excess of the carbonyl component was used to diminish the amount of the unwanted bis-ketimine product formed. A small amount of the respective bis(iminoethyl)pyridine side product could be removed by treatment with an ethanol/THF (2:1) mixture at reflux temperatures. Subsequently, **3** was then reacted with the alkenylamines **4a–d**⁸ in methanol at 60 °C (16 h) to give the unsymmetrical chelate ligands **5a–d** in good yield (64–82%, see Scheme 2). The products crystallized readily from solution at 0 °C.

Scheme 2



The ligand systems show very typical NMR data. Figure 1 shows the ^1H NMR spectrum of **5d**. It features three separate pyridine resonances, a pair of aromatic CH signals of the N-aryl

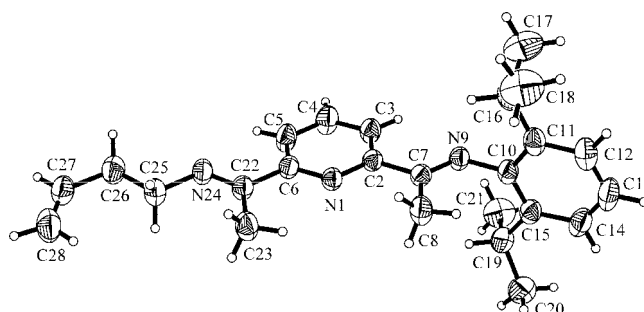


Figure 2. Molecular geometry of **5b**.

substituent, the typical resonances of the terminal vinyl group, and four multiplets corresponding to the tetramethylene tether. There are two singlets resulting from the iminoethyl methyl groups and one septet of 2H intensity corresponding to the isopropyl methine groups. The isopropyl methyl groups give rise to a pair of doublets (each of 6H intensity). This indicates an orthogonal orientation of the diisopropylphenyl substituent at nitrogen relative to the central bis(iminoethyl)pyridine plane. The resulting element of axial prochirality renders the isopropyl methyl group pairwise diastereotopic.⁹ Systems **5a–c** feature similar NMR spectra (for details see the Experimental Section and the Supporting Information).

All chelate ligand systems **5a–c** were characterized by X-ray diffraction. These X-ray crystal structure analyses confirmed the axially prochiral geometries that were assumed from the NMR analysis. The structures of all three compounds are very similar. Therefore, it will suffice to present and discuss the solid state structure of the butenyl-substituted compound **5b** as a typical example. Details of the remaining compounds **5a,c** are found in the Experimental Section and the Supporting Information.

In the crystal state compound **5b** features a planar core that extends through both C=N units. The overall conformation is of an extended W shape (see Figure 2). Both imino C=N bonds are oriented coplanar with the central pyridine ring. They feature dihedral angles of 179.6(1)° for N1–C2–C7–N9 and 172.9(1)° for N1–C6–C22–N24. Both imino groups are in the *E* configuration (dihedral angles C2–C7–N9–C10 = 178.8(1)°, C6–C22–N24–C25 = 178.3(1)°). The plane of the 2,6-diisopropylphenyl substituent at N9 is oriented in an orthogonal position relative to the bis(iminoethyl)pyridine ligand core (dihedral angle C7–N9–C10–C11 = 90.8(2)°). Both of the imino C=N bonds are short (C7–C9 = 1.280(2) Å, C22–N24 = 1.278(2) Å).¹⁰

For comparison we have also synthesized the saturated *n*-butyl analogue of **5b**: namely, compound **6b** (see Scheme 3). This

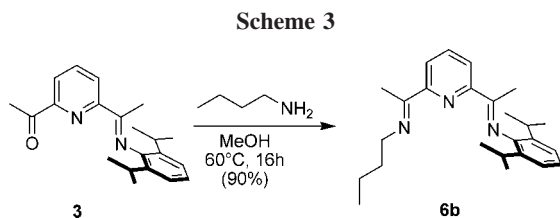
(7) Layer, R. W. *Chem. Rev.* **1963**, *63*, 489–510.

Table 1. Selected Structural Data of the Complexes 7a–d (Co), 8c (Fe), and 11a (Co)^a

	7a	7b	7c	7d	8c	11a
M/n	Co/1	Co/2	Co/3	Co/4	Fe/3	Co/1
M–C11	2.305(2)	2.302(1)	2.268(1)	2.279(1)	2.299(2)	
M–Cl2	2.272(1)	2.281(1)	2.270(1)	2.274(1)	2.281(2)	1.949(2) ^b
C11–M–Cl2	119.3(1)	119.3(1)	120.3(1)	118.9(1)	120.3(1)	
M–N1	2.043(4)	2.050(2)	2.043(2)	2.047(3)	2.072(5)	1.818(2)
M–N9	2.215(4)	2.229(2)	2.253(2)	2.245(3)	2.256(5)	1.900(2)
M–N24	2.163(5)	2.164(2)	2.140(3)	2.161(3)	2.166(6)	1.899(2)
C7–N9	1.274(7)	1.283(2)	1.273(4)	1.282(5)	1.279(8)	1.324(3)
C22–N24	1.290(7)	1.281(3)	1.286(4)	1.283(5)	1.292(8)	1.316(3)
N1–M–C11	93.4(1)	96.9(1)	98.8(1)	94.5(1)	98.7(2)	
N1–M–Cl2	147.3(1)	143.8(1)	140.9(1)	146.6(1)	141.1(1)	172.4(1) ^c
N1–M–N9	74.2(2)	74.3(1)	74.0(1)	74.1(1)	73.2(2)	81.0(1)
N1–M–N24	74.8(2)	74.8(1)	75.9(1)	75.2(1)	74.2(2)	81.1(1)
N9–M–Cl2	98.3(1)	98.1(1)	96.8(1)	96.7(1)	98.1(1)	100.4(1) ^c
N24–M–Cl2	97.6(1)	97.1(1)	100.1(1)	98.7(1)	101.4(2)	97.8(1) ^c
N24–M–N9	143.6(2)	144.9(1)	148.2(1)	144.0(1)	146.1(2)	161.7(1)
C2–C7–N9–C10	178.5(4)	175.3(2)	–171.6(3)	173.4(3)	171.2(5)	178.1(2)
C7–N9–C10–C11	–96.1(6)	88.6(2)	–85.2(4)	83.1(5)	86.6(8)	86.0(3)
C7–N9–C10–C15	85.6(6)	–92.6(2)	95.6(3)	–97.8(4)	–94.4(7)	–97.1(2)

^a Bond lengths are given in Å and bond angles and dihedral angles in deg. ^b Co–CH₃. ^c N–Co–CH₃.

was obtained from the reaction of compound **3** with *n*-butylamine under conditions analogous to those described above. It was isolated in 90% yield. Compound **6b** was also characterized by an X-ray crystal structure analysis. It shows features similar to those found for the unsaturated analogues **5a–d** (for details see the Experimental Section and the Supporting Information).



Synthesis and Characterization of the Bis(iminoethyl)pyridine Cobalt and Iron Complexes. We reacted each of the new ligand systems **5a–d** with anhydrous CoCl₂ and with FeCl₂, respectively. The corresponding chelate MCl₂ complexes (M = Co, **7a–d**; M = Fe, **8a–d**) were obtained as green (Co(II)) or blue (Fe(II)) paramagnetic solids in yields ranging between 60% (**8d**) and 99% (**7b**). All four cobalt complexes **7a–d** and the iron complex **8c** were characterized by X-ray diffraction. We have also carried out an X-ray crystal structure analysis of the iron complex **8b**, which confirmed the proposed structure (see the Supporting Information), but due to its rather large *R* factor of 9%, details of this structure will not be discussed here. We have also prepared the cobalt and iron complexes **9b** and **10b**, derived from the “saturated” ligand **6b**, for comparison (ca. 99% yield, see Scheme 4).

The iron complex **8c** features a structure that is located somewhere between a distorted square pyramidal and a strongly distorted trigonal bipyramidal coordination geometry of the metal. The Fe–C11 bond is slightly longer than the Fe–Cl2 bond ($\Delta d \approx 0.02$ Å). Both of the imine C=N bonds in **8c** are rather short (1.279(8) and 1.292(8) Å). The Fe–imine nitrogen bonds are markedly larger than the central Fe–pyridine nitrogen bond (2.256(5)/2.166(6) Å vs 2.072(5) Å). The central N₃Fe unit is very close to coplanar (dihedral angles N1–C6–C22–N24 = 0.7(9)°, N1–C2–C7–N9 = 2.0(8)°). The pentenyl substituent at N24 is found in a fully extended conformation. The bulky

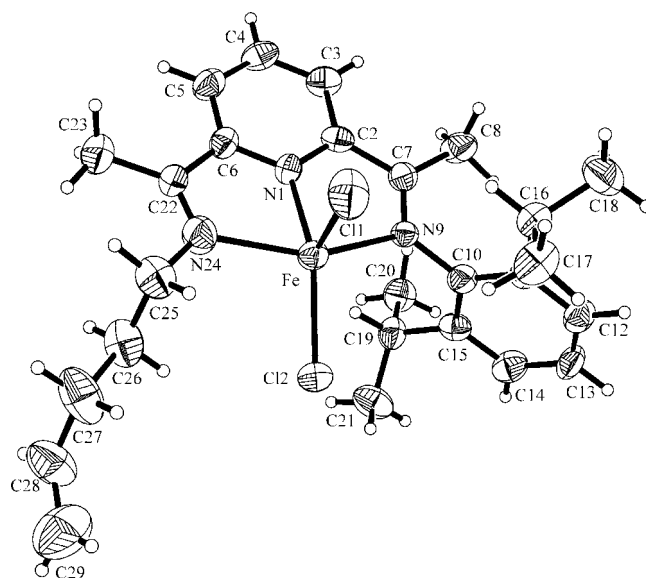


Figure 3. Molecular geometry of the Fe complex **8c**.

2,6-diisopropylphenyl substituent at N9 is rotated perpendicular to the central chelate ligand plane (see Table 1 and Figure 3).¹¹

Figure 4 shows the molecular structure of the cobalt complex **7b** as a typical example of the **7a–d** series. The overall structural arrangement is analogous to that of the iron complex **8c** (see Table 1). The C11–Co–Cl2 angle here amounts to 119.3(1)°, and the pyridine N1–Co–C11 angle is close to normal (96.9(1)°). Again, the 2,6-diisopropylphenyl group at N9 is rotated to stand perpendicular to the central chelate ligand plane. The allyl end group of the butenyl substituent at the other imino group is also rotated markedly. The structural features

(8) The alkenylamine synthesis is analogous to those in: (a) Ettliger, M. G.; Hodgkins, J. E. *J. Am. Chem. Soc.* **1955**, *77*, 1831–1836 (*N*-(4-pentenyl)phthalimide). (b) Sato, T.; Nakamura, N.; Ikeda, K.; Okada, M.; Ishibashi, H.; Ikeda, M. *J. Chem. Soc., Perkin Trans. 1* **1992**, 2399–2407(3-butenylamine). (c) Gagné, M. R.; Stern, C. L.; Marks, T. J. *J. Am. Chem. Soc.* **1992**, *114*, 275–294(4-pentenylamine).

(9) Eliel, E. L.; Wilen, S. H.; Mander, L. N. *Stereochemistry of Organic Compounds*; Wiley-VCH: New York, 1994; Chapter 14.

(10) Allen, F. H.; Kennard, O.; Watson, D. G.; Brammer, L.; Orpen, A. G.; Taylor, R. *J. Chem. Soc., Perkin Trans. 2* **1987**, S1–S19.

(11) See, for a comparison: (a) Cámpora, J.; Naz, A. N.; Palma, P.; Rodríguez-Delgado, A.; Álvarez, E.; Tritto, I.; Boggioni, L. *Eur. J. Inorg. Chem.* **2008**, 1871–1879.

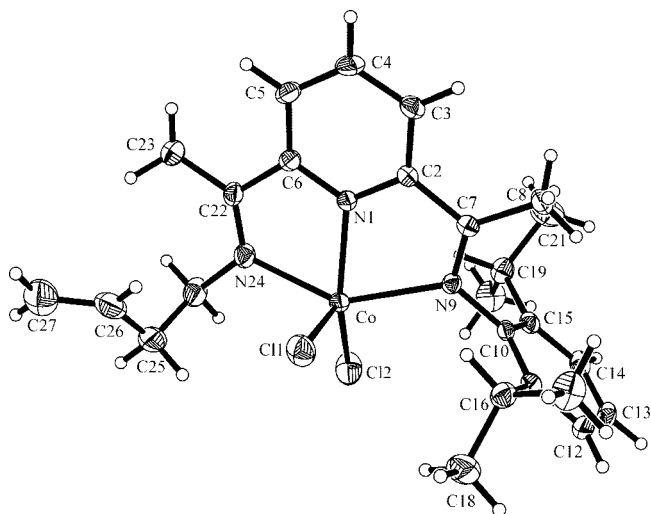


Figure 4. View of the molecular structure of the cobalt complex **7b**.

of the remaining three examples (**7a,c,d**) in this series are very similar (see Table 1 and the Supporting Information for further details).^{12,13}

Treatment of the paramagnetic cobalt dichloride complex **7a** with an excess of methyllithium (3 equiv) yielded the diamagnetic cobalt(I) methyl complex **11a** (89% isolated; Scheme 5).^{14,15} The ¹H NMR spectrum of **11a** (Figure 5) shows some rather extraordinary features, such as the signal of the central pyridine hydrogen 4-H at very a high δ value of 10.10 and the pair of ketimine CH₃ signals at negative δ values (-0.64 , -1.51). This may indicate an electronic structure of **11a** similar to those discussed by Budzelaar et al.¹⁶ for related systems comprised of a low-spin cobalt(II) state antiferromagnetically coupled with the radical anion of the ligand. The redox reaction would in this interpretation have involved the noninnocent ligand. The Co–CH₃ ¹H NMR resonance of complex **11a** was located at δ 0.54.

Complex **11a** was also characterized by an X-ray crystal structure analysis (see Figure 6 and Table 1). The cobalt center in complex **11a** exhibits a distorted-square-planar coordination geometry (N1–Co–C1 = 172.4(1)°, N24–Co–N9 = 161.7(1)°). It features a Co–CH₃ group (1.949(2) Å) trans to the pyridine nitrogen atom. The bonding features of the chelate ligand–Co

(12) (a) Britovsek, G. J. P.; Gibson, V. C.; Hoarau, O. D.; Spitzmesser, S. K.; White, A. J. P.; Williams, D. J. *Inorg. Chem.* **2003**, *42*, 3454–3465. (b) Britovsek, G. J. P.; Mastroianni, S.; Solan, G. A.; Baugh, S. P. D.; Redshaw, C.; Gibson, V. C.; White, A. J. P.; Williams, D. J.; Elsegood, M. R. J. *Chem. Eur. J.* **2000**, *6*, 2221–2231. (c) Britovsek, G. J. P.; Gibson, V. C.; Kimberley, B. S.; Mastroianni, S.; Redshaw, C.; Solan, G. A.; White, A. J. P.; Williams, D. J. *Dalton Trans.* **2001**, 1639–1644. (d) Gibson, V. C.; Tellmann, K. P.; Humphries, M. J.; Wass, D. F. *Chem. Commun.* **2002**, 2316–2317.

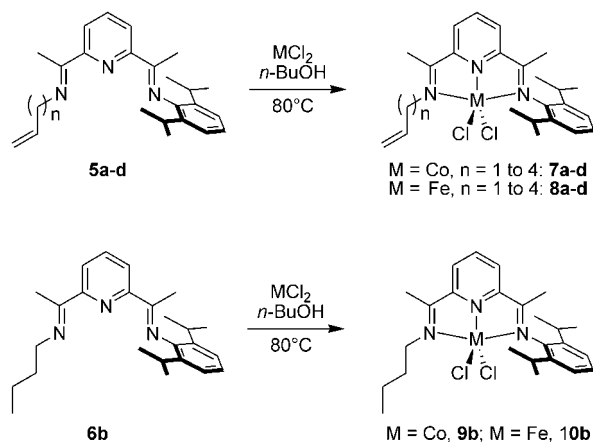
(13) (a) Reardon, D.; Conan, F.; Gambarotta, S.; Yap, G.; Wang, Q. *J. Am. Chem. Soc.* **1999**, *121*, 9318–9325. (b) Dias, E. L.; Brookhart, M.; White, P. S. *Chem. Commun.* **2001**, 423–424. (c) Esteruelas, M. A.; Lopez, A. M.; Mendez, L.; Oliván, M.; Onate, E. *Organometallics* **2003**, *22*, 395–406. (d) Calderazzo, F.; Englert, U.; Pampaloni, G.; Santi, R.; Sommazzi, A.; Zinna, M. *Dalton Trans.* **2005**, 914–922.

(14) (a) Kooistra, T. M.; Knijnenburg, Q.; Smits, J. M. M.; Horton, A. D.; Budzelaar, P. H. M.; Gal, A. W. *Angew. Chem.* **2001**, *113*, 4855–4858; *Angew. Chem., Int. Ed.* **2001**, *40*, 4719–4722. (b) Gibson, V. C.; Humphries, M. J.; Tellmann, K. P.; Wass, D. F.; White, A. J. P.; Williams, D. J. *Chem. Commun.* **2001**, 2252–2253.

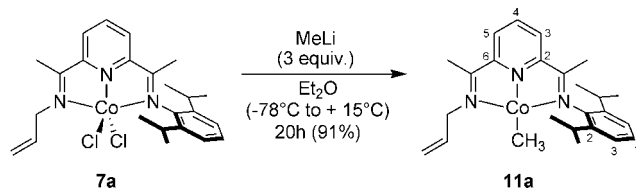
(15) Kleigrewe, N.; Steffen, W.; Blömker, T.; Kehr, G.; Fröhlich, R.; Wibbeling, B.; Erker, G.; Wasilke, J. C.; Wu, G.; Bazan, G. C. *J. Am. Chem. Soc.* **2005**, *127*, 13955–13968.

(16) Knijnenburg, Q.; Hetterscheld, D.; Kooistra, T. M.; Budzelaar, P. H. M. *Eur. J. Inorg. Chem.* **2004**, 1204–1211.

Scheme 4



Scheme 5



moiety are markedly different from those of the pentacoordinated Co(II) systems (**7a–d**; see Table 1). In **11a** the bonds of cobalt to all three nitrogen atoms are much shorter than in **7**. The shortest is the Co–pyridine linkage at 1.818(2) Å (Co–N1), but the Co–N(imine) bonds are also very short (Co–N9 = 1.900(2) Å, Co–N24 = 1.899(2) Å). In **11a** the imine ligand–cobalt donor bonds are stronger than in **7**, but at the same time there seems to be substantially increased metal to ligand back-bonding. Consequently, the imine C=N bond lengths are substantially increased (C7–N9 = 1.324(3) Å, C22–N24 = 1.316(3) Å) relative to **7** ($\Delta d \approx 0.04$ Å) and the adjacent C2–C7 (1.428(3) Å) and C6–C22 (1.440(3) Å) imine connections to the pyridine ring decreased ($\Delta d \approx 0.05$ Å). As expected, the bulky 2,6-diisopropylphenyl substituent at N9 is found in an orthogonal conformation. The vinyl end group of the allyl substituent at the other imine nitrogen center (N24) is also rotated normal to the central chelate ligand plane (C22–N24–C25–C26 = 90.8(3)°).

Ethene Oligomerization and Polymerization. The metal complexes described above in this study were briefly tested for their ethene polymerization activities. Activation was carried out by treatment with methylalumoxane, employing an Al:M ratio of 300:1.¹⁷ The catalytic reactions were carried out in toluene solution at room temperature in a Büchi autoclave system using a pressure of 2 bar of ethene. In several experiments it was found that preactivation of the metal complexes with MAO gave increased activities. All of the cobalt complexes gave relatively low catalyst activities (for details see the Supporting Information). The highest activities were found with the systems **7a**/MAO (activity ~ 60 g of polyethylene/(mmol of cat.) (bar of ethene) h) and **11a**/MAO (activity

(17) This seems to be an optimal ratio for such systems; see, e.g.: Britovsek, G. J. P.; Bruce, M.; Gibson, V. C.; Kimberley, B. S.; Maddox, P. J.; Mastroianni, S.; McTavish, S. J.; Redshaw, C.; Solan, G. A.; Strömberg, S.; White, A. J. P.; Williams, D. J. *J. Am. Chem. Soc.* **1999**, *121*, 8728–8740.

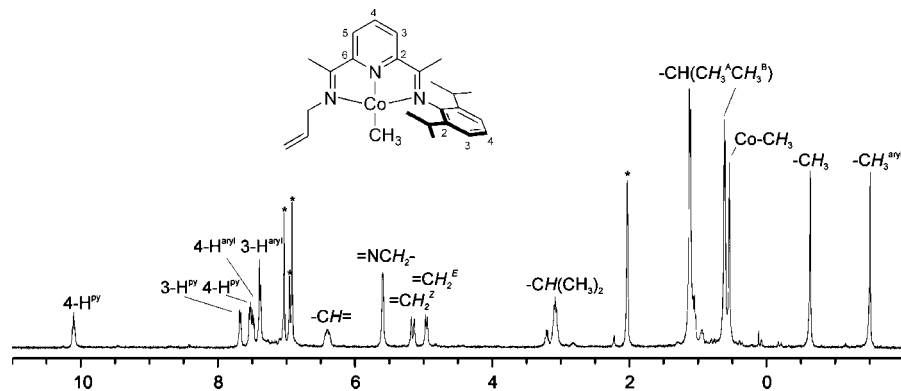


Figure 5. ^1H NMR spectrum of complex **11a** (d_8 -toluene (*), 400 MHz, 298 K; aryl = 2,6-diisopropylphenyl).

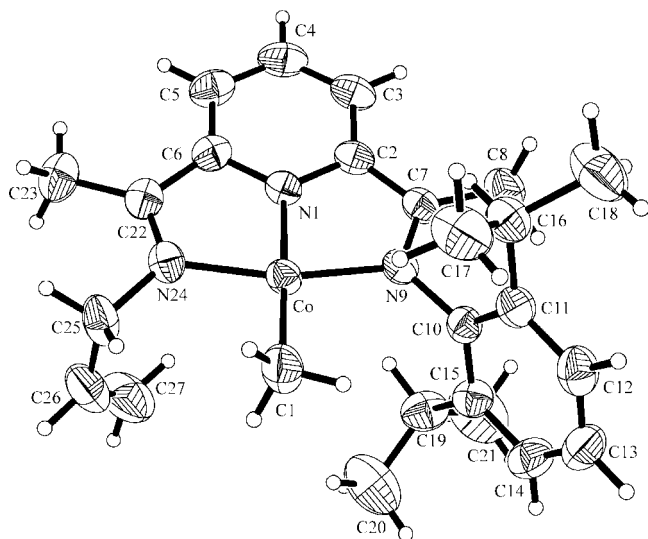


Figure 6. Projection of the molecular geometry of the cobalt complex **11a**.

~ 90).¹⁸ In all cases for the cobalt-derived catalyst systems **7**/MAO or **11**/MAO linear polyethylene was obtained.

The situation with the iron catalysts is somewhat different. Treatment of the *N*-allyl iron complex **8a** with MAO gave a rather active catalyst system, as expected.¹⁹ With the preactivated catalyst an overall activity of ~ 470 was observed; direct

(18) The [Co]–CH₃ system apparently requires a special activation mechanism; see, e.g. Jin, J.; Wilson, D. R.; Chen, E. Y.-X. *Chem. Commun.* **2002**, 708–709.

(19) There is a controversial discussion about the actual active species formed in the (N,N,N)-chelate ligand)FeCl₂ + MAO catalyst system; see e.g.: (a) De Bruin, B.; Bill, E.; Bothe, E.; Weyhermüller, T.; Wieghardt, K. *Inorg. Chem.* **2000**, *39*, 2936–2947. (b) Britovsek, G. P. J.; ClentSmith, G. K. B.; Gibson, V. C.; Goodgame, D. M. L.; McTavish, S. J.; Pankhurst, Q. A. *Catal. Commun.* **2002**, *3*, 207–211. (c) Britovsek, G. P. J.; Gibson, V. C.; Spitzmesser, S. K.; Tellmann, K. P.; White, A. J. P.; Williams, D. J. *Dalton Trans.* **2002**, 1159–1171. (d) Enright, D.; Gambarotta, S.; Yap, G. P. A.; Budzelaar, P. H. M. *Angew. Chem.* **2002**, *114*, 3309–3312; *Angew. Chem., Int. Ed.* **2002**, *41*, 4029–4032. (e) Bryliakov, K. P.; Semikolenova, N. V.; Zudin, V. N.; Zakharov, V. A.; Talsi, E. P. *Cat. Commun.* **2004**, *5*, 45–48. (f) Bryliakov, K. P.; Semikolenova, N. V.; Zakharov, V. A.; Talsi, E. P. *Organometallics* **2004**, *23*, 5375–5378. (g) Cámpora, J.; Naz, A. M.; Palma, P.; Álvarez, E.; Reyes, M. L. *Organometallics* **2005**, *24*, 4878–4871. (h) Scott, J.; Gambarotta, S.; Korobkov, I.; Budzelaar, P. H. M. *Organometallics* **2005**, *24*, 6298–6300. (i) Bouwkamp, M. W.; Lobkovsky, E.; Chirik, P. J. *J. Am. Chem. Soc.* **2005**, *127*, 6298–6300. (j) Scott, J.; Gambarotta, S.; Korobkov, I.; Budzelaar, P. H. M. *J. Am. Chem. Soc.* **2005**, *127*, 13019–13029. (k) Bart, S. C.; Chlopek, K.; Bill, E.; Bouwkamp, M. W.; Lobkovsky, E.; Neese, F.; Wieghardt, K.; Chirik, P. J. *J. Am. Chem. Soc.* **2006**, *128*, 13901–13912. (l) Fernández, I.; Trovitch, R. J.; Lobkovsky, E.; Chirik, P. J. *Organometallics* **2008**, *27*, 109–118.

Table 2. Ethene Polymerization and Oligomerization at the Iron Catalyst Systems **8**/MAO^a

compd	t (min)	amt of PE (g)	mp (°C)	amt of olig (g)	M_n^c	PDI	activity ^d
8a	30	17.8	125	5.5	288	1.28	466
8a^b	30	15.3	124	5.7	310	1.15	419
8b	60	1.7	121	4.8	256	1.23	65
8c	60	0.5	120	6.4	236	1.27	69
8d	60	5.9	124	2.4	231	1.23	83
10b	60	0.9	119	12.8	247	1.31	137

^a Conditions: 2 bar of ethene, 25 °C, 200 mL of toluene, Al:Fe = 300, 0.05 mmol of Fe complex, preactivated catalysts used. ^b Without preactivation. ^c Molecular weight of the oligomer fraction. ^d Total activity (PE + oligomers), in units of g of PE + olig./((mmol of Fe) h (bar of ethene)).

activation in the Büchi autoclave gave only a slightly less active catalyst (activity ~ 420). The reaction produced a mixture of polyethylene (shown to be linear PE by NMR and DSC) and a substantial oligomeric fraction. The low-molecular-weight oligomers were separated from the high-molecular-weight polyethylene by extraction. They were analyzed by GPC and shown to comprise a mixture of ca. 10- to 15-mers with a relatively narrow molecular weight distribution (PDI ≈ 1.2 –1.3).

As expected, this is in stark contrast to the behavior of the catalyst derived from the saturated *N*-(*n*-butyl) iron complex **10b**. Its treatment with MAO gave a slightly less active catalyst (activity ~ 130) that produced mostly oligoethylenes (12.8 g isolated after 60 min of reaction time) and only a very minor amount of polyethylene (0.9 g) (cf. **8a**/MAO: 5.5 g of oligomers and 17.8 g of polyethylene after 30 min reaction time). The remaining catalyst systems **8b**–**d**/MAO fall between these extremes: they all produce mixtures of the C₁₀–C₁₅ oligoethylenes with mostly substantial amounts of polyethylene (see Table 2).

We actually expected that the catalysts derived from the unsymmetrical Fe chelate complexes **8**, featuring a rather small linear alkenyl substituent at one of the imine nitrogen atoms, would behave similar to the “Bianchini catalysts” (e.g., **2**/MAO)⁵ and produce only low-molecular-weight linear ethene oligomers. Our saturated example (**10b**/MAO) behaves just like that, but some of the unsaturated systems **8**/MAO show a strongly

(20) For remotely related examples, see e.g.: (a) Peifer, B.; Milius, W.; Alt, H. G. *J. Organomet. Chem.* **1998**, *553*, 205–220. (b) Kaul, F. A. R.; Puchta, G. T.; Schneider, H.; Bielert, F.; Mihalios, D.; Herrmann, W. A. *Organometallics* **2002**, *21*, 74–82. (c) Licht, A. I.; Alt, H. G. *J. Organomet. Chem.* **2002**, *648*, 134–148. (d) Zhu, H.; Jin, G.-X.; Hu, N. J. *Organomet. Chem.* **2002**, *655*, 167–171. (e) Licht, A. I.; Alt, H. G. *J. Organomet. Chem.* **2003**, *687*, 142–152. (f) Gómez-Ruiz, S.; Polo-Cerón, D.; Prashar, S.; Fajardo, M.; Antónolo, A.; Otero, A. *Eur. J. Inorg. Chem.* **2007**, 4445–4455.

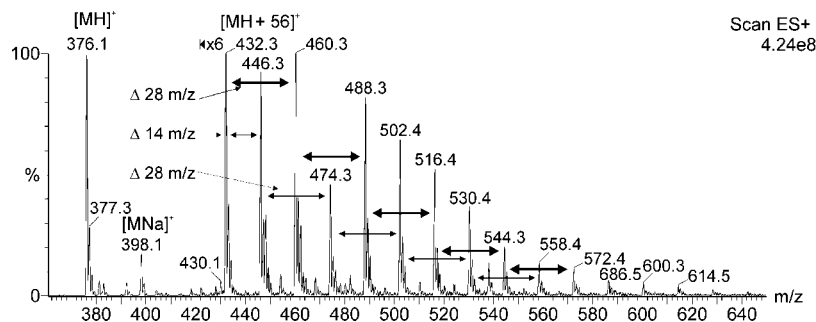


Figure 7. ESI⁺ MS spectrum of the free ligands obtained after CH₃OH quenching of an ethylene polymerization reaction mixture at the **8b**/MAO catalyst.

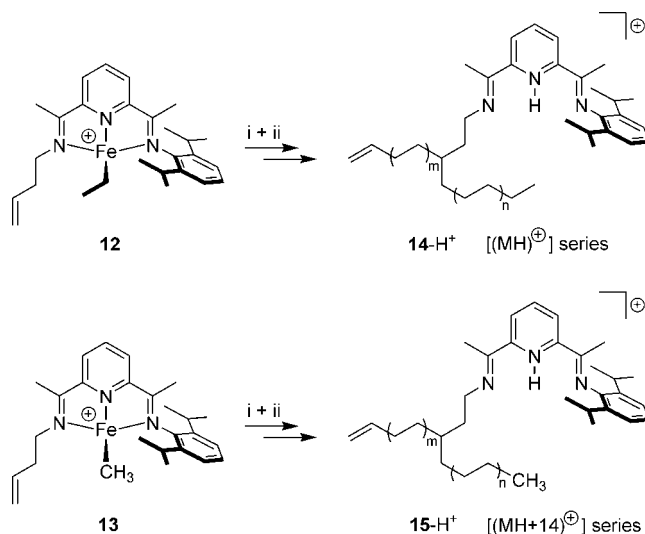
deviating behavior. At present it is far from being clear as to what this special catalytic behavior of the systems **8** might have caused. Since the steric bulk of the unsaturated groups at the imine nitrogen is practically the same as for their saturated analogues, we are tempted to speculate that a secondary reaction of the pendant alkenyl group during the oligomerization reaction might have caused the observed unusual behavior. An alkenyl-specific reaction could potentially be the involvement of the pendant alkenyl functionality in the actual oligomerization reaction sequence.^{20,21} A noninnocent behavior of the pendant alkenyl moieties could possibly lead to a conversion of these substituents to a much larger and much more bulky oligoethylene substituent at that imine nitrogen center, thereby potentially altering the chain termination and chain transfer properties of the catalyst during the actual olefin oligomerization process toward the direction of polyethylene formation.

One can devise a variety of experiments to study the question of the active involvement of the pendant alkenyl group. At this time we have only started to investigate the potential “noninnocent” behavior of an alkenyl substituent at the imine nitrogen and carried out the following experiments: the systems **8** were reacted with ethene (1 bar) in THF in a Schlenk flask upon treatment with 250 equiv of MAO. After 30 min the mixture was quenched by the addition of methanol. This procedure destroyed the Fe complexes and liberated the free ligands. These were then analyzed by ESI MS.²² In the case of the reaction of **8b** (R = *n*-butenyl) we recorded the mass spectrum depicted in Figure 7.

In this ESI⁺ MS spectrum (see Figure 7) we observe the protonated ligand system **5b** + H⁺ (MH⁺: *m/z* 376) and the corresponding **5b** + Na⁺ (MNa⁺: *m/z* 398) feature. Then we monitor two systematic series of signals. The first begins at *m/z* 432 (MH⁺ + 56) (i.e., ligand plus two ethene units). We see a sequence of signals derived from this by the addition of the third ethene monomer (gives *m/z* 460), the fourth (*m/z* 488), and so forth. It is conceivable that this series of compounds (**14-H⁺**) might be derived from the involvement of the pendant olefinic unit at the active catalyst stage in the polymerization process.

The second systematic series of features in the ESI⁺ MS spectrum of this specific experiment is offset from the signals of the first by 14 mass units. A competing sequence starting, for example, from **13** (either generated in the initial activation

Scheme 6



i ethene polymerization conditions (MAO, C₂H₄)
ii quenching with methanol

procedure or obtained in situ by chain transfer to/from aluminum) could account for the (MH⁺ + 14) series.

The formation of possible structures (**14-H⁺**, **15-H⁺**) can be formulated using the “rules” of α -olefin insertion at the bis(iminoalkyl)pyridine iron catalysts as they were deduced by Brookhart et al.²³ (see Scheme 6; a detailed scheme is provided with the Supporting Information).^{20,24}

Some Conclusions

The cobalt and iron chelate complexes **7** and **8** are readily obtained by treatment of the neutral ligand systems **5** with CoCl₂ and FeCl₂, respectively. The structures of these paramagnetic complexes are rather unexceptional. Both series (Co and Fe) feature typical strongly distorted square pyramidal/trigonal

(23) Small, B. L.; Brookhart, M. *Macromolecules* **1999**, *32*, 2120–2130.

(21) The oligomers feature vinyl groups in their ¹³C NMR spectra. Therefore, we assume that chain transfer to aluminum probably has not played a dominating role in these experiments.

(22) For some remotely related MS studies of active Ziegler–Natta catalyst systems: (a) Chen, P. *Angew. Chem.* **2003**, *115*, 2938–2954; *Angew. Chem., Int. Ed.* **2003**, *42*, 2832–2847. (b) Di Lena, F.; Quintanilla, E.; Chen, P. *Chem. Commun.* **2005**, 5757–5759, and references cited therein.

(24) There is principally the possibility of ligand methylation by, for example, trimethylaluminum in such systems; see, e.g.: (a) Bruce, M.; Gibson, V. C.; Redshaw, C.; Solan, G. A.; White, A. J. P.; Williams, D. J. *Chem. Commun.* **1998**, 2523–2524. (b) Knijnenburg, Q.; Smits, J. M. M.; Budzelaar, P. H. M. *Organometallics* **2006**, *25*, 1036–1046. See also: (c) Clentsmith, G. K. B.; Gibson, V. C.; Hitchcock, P. B.; Kimberley, B. S.; Rees, C. W. *Chem. Commun.* **2002**, 1498–1499. (d) Sugiyama, H.; Aharonian, G.; Gambarotta, S.; Yap, G. P. A.; Budzelaar, P. H. M. *J. Am. Chem. Soc.* **2002**, *124*, 12268–12274. (e) Tsurugi, H.; Matsuo, A.; Yamagata, T.; Mashima, K. *Organometallics* **2004**, *23*, 2797–2805. (f) Sugiyama, H.; Gambarotta, S.; Yap, G. P. A.; Wilson, D. R.; Thiele, S. K.-H. *Organometallics* **2004**, *23*, 5053–5061. (g) Blackmore, I. J.; Gibson, V. C.; Hitchcock, P. B.; Rees, C. W.; Williams, D. J.; White, A. J. P. *J. Am. Chem. Soc.* **2005**, 6012–6020.

bipyramidal geometries. The pendant alkenyl substituents do not show any direct interaction with the metal at the $[M]Cl_2$ complex state. Also, the formation of the cobalt(I) methyl complex **11a** is typical. Several other examples of this reaction type were previously described in the literature.^{14,15} These apparently quite normal and unexceptional systems behave rather exceptionally at their active homogeneous Ziegler–Natta catalyst stage. For both series we would have expected just ethylene oligomer formation,⁵ but not polyethylene production, if the pendant olefinic group at the ligand framework would have been just a nonparticipating bystander. We would have expected a catalyst behavior similar to that of the related previously described “Bianchini systems” (**2** and its congeners).⁵ In contrast, we observe polyethylene formation to take place at most of the N-alkenyl chelate cobalt complexes **7/MAO** and a very interesting competition between polyethylene and oligoethylene product formation at the **8/MAO**-derived catalyst systems. In these cases the molecular weight and the molecular weight distribution of the oligoethylene product fraction are similar to those for the oligomers described as being formed at the reference systems (**2/MAO**, **10b/MAO**). This indicates that the olefinic substituents attached at the imine nitrogen atoms of our new ligand systems are not inert—they seem to be “noninnocent” substituents that show a tendency of becoming involved in the oligomerization process and thereby of controlling it. The very nature of this interaction and involvement is, however, not completely clear at this time. One might envisage that the vinyl end group might, for example, just reversibly coordinate to the metal center at the active catalyst stage and thereby alter the chain termination and transfer probabilities and behavior. In view of our **8b/MAO** experiment and the corresponding ESI⁺ MS analysis (see Figure 7 and the text) there might be a good chance that the vinyl end group of the ligand substituent can actually actively take part in the polymerization process as an internal comonomer^{20,22} and thereby alter the overall features of the catalyst during the oligomerization/polymerization process. In either case it seems that the pendant alkenyl moieties at the chelate ligand framework of these interesting new complex systems are able to exert an internal dynamic control on the characteristic chemical features of these active olefin oligomerization and polymerization catalysts.

Experimental Section

General Procedures. Reactions with air- and water-sensitive compounds were carried out under argon using Schlenk-type glassware or in a glovebox. Solid compounds were collected on sintered-glass frits and washed with appropriate solvents before being dried under vacuum. Solvents were dried and distilled under argon prior to use. Compound **3**⁵ and the alkenylamines **4b–d**⁸ were prepared analogously as described in the literature. 2,6-Diacetylpyridine, 2,6-diisopropylaniline, and allylamine **4a** were used as purchased from commercial suppliers. The following instruments were used for physical characterization of the compounds. Melting points: DSC 2010 TA instruments. Elemental analyses: Foss-Heraeus CHNO-Rapid. ESI-MS analysis: Quattro LCZ (Waters Micromass, Manchester, U.K.) equipped with a nano spray inlet. IR: FT-IR spectrometer Excalibur 3100 (Varian) equipped with a Specac Golden Gate ATR MK II unit. NMR: Bruker AC 200 P (¹H, 200.1 MHz; ¹³C, 50.3 MHz), AMX 400 (¹H, 400.1 MHz; ¹³C, 100.6 MHz), Varian UNITY plus NMR spectrometer (¹H, 599.1 MHz; ¹³C, 150.7 MHz). Assignments of the resonances were supported by 2D experiments.

X-ray Crystal Structure Analyses. Data sets were collected with Enraf-Nonius CAD4 and Nonius KappaCCD diffractometers, in case of Mo radiation with a rotating anode generator. Programs

used: data collection EXPRESS (Nonius BV, 1994) and COLLECT (Nonius BV, 1998), data reduction MolEN (K. Fair, Enraf-Nonius BV, 1990) and Denzo-SMN (Otwinowski, Z.; Minor, W. Methods Enzymol. 1997, 276, 307–326), absorption correction for CCD data SORTAV (Blessing, R. H. Acta Crystallogr. 1995, A51, 33–37; Blessing, R. H. J. Appl. Crystallogr. 1997, 30, 421–426) and Denzo (Otwinowski, Z.; Borek, D.; Majewski, W.; Minor, W. Acta Crystallogr. 2003, A59, 228–234), structure solution SHELXS-97 (Sheldrick, G. M. Acta Crystallogr. 1990, A46, 467–473), structure refinement SHELXL-97 (Sheldrick, G. M. Acta Crystallogr. 2008, A64, 112–122), graphics XP (BrukerAXS, 2000).

General Procedure for the Preparation of the Unsymmetrical Ligand Systems 5a–d and 6b. In a flame-dried Schlenk flask a mixture of compound **3** in methanol and the appropriate alkenylamine was heated at 60 °C under stirring for 20 h. The hot yellow solution was filtered under an argon atmosphere to remove the insoluble symmetrical side product 2,6-bis(*N*-(2,6-diisopropylphenyl)iminoethyl)pyridine. After half of the solvent was removed, the resulting solution was kept at 0 °C for 24 h. The desired product precipitated as yellow crystals, which were separated by filtration. A second crop of product was obtained from the mother liquor after reducing the solvent volume and cooling to 0 °C for 24 h. In the solid state the ligand systems are air-stable; to protect them against moisture they were stored in a glovebox.

Preparation of Ligand 5a. A sample of **3** (3.47 g, 10.8 mmol) in 50 mL of methanol was treated with allylamine (**4a**; 8.08 mL, 6.14 g, 107.6 mmol, 10 equiv) to yield a light yellow solid (79%, 3.10 g, 8.60 mmol). Mp (DSC): 111 °C. MS-ESI (MeOH, ES⁺): *m/z* 384.2 ($[M + Na]^+$), 362.2 ($[M + H]^+$). Anal. Calcd for C₂₄H₃₁N₃ (361.52): C, 79.73; H, 8.64; N, 11.62. Found: C, 79.71; H, 8.61; N, 11.57. ¹H NMR (*d*₂-dichloromethane, 600 MHz, 298 K): δ(¹H) 8.37 (dd, ³*J* = 7.8 Hz, ⁴*J* = 1.0 Hz, 1H, 3-HPy), 8.25 (dd, ³*J* = 7.8 Hz, ⁴*J* = 1.0 Hz, 1H, 5-HPy), 7.84 (t, ³*J* = 7.8 Hz, 1H, 4-HPy), 7.16 (m, 2H, 3-H^{aryl}), 7.08 (m, 1H, 4-H^{aryl}), 6.16 (ddt, ³*J* = 17.3 Hz, ³*J* = 10.3 Hz, ³*J* = 5.2 Hz, 1H, =CH=), 5.32 (dq, ³*J* = 17.3 Hz, ⁴*J* = ²*J* = 1.8 Hz, 1H, =CH₂²), 5.17 (dq, ³*J* = 10.3 Hz, ⁴*J* = ²*J* = 1.8 Hz, 1H, =CH₂⁵), 4.23 (m, 2H, =NCH₂-), 2.75 (sept, ³*J* = 6.9 Hz, 2H, -CH(CH₃)₂), 2.42 (s, 3H, -CH₃^{alkyl}), 2.23 (s, 3H, -CH₃^{aryl}), 1.15 (d, ³*J* = 6.9 Hz, 6H, -CH(CH₃^ACH₃^B)), 1.13 (d, ³*J* = 6.9 Hz, 6H, -CH(CH₃^ACH₃^B)). ¹³C{¹H} NMR (*d*₂-dichloromethane, 150 MHz, 298 K): δ(¹³C) 167.5 (N=C^{aryl}), 167.4 (N=C^{alkyl}), 156.8 (C-6^{py}), 155.2 (C-2^{py}), 147.0 (C-1^{aryl}), 137.0 (C-4^{py}), 136.7 (-CH=), 136.2 (C-2^{aryl}), 123.8 (C-4^{aryl}), 123.3 (C-3^{aryl}), 122.1 (C-5^{py}), 121.8 (C-3^{py}), 115.1 (=CH₂), 55.2 (=NCH₂-), 28.6 (-CH(CH₃)₂), 23.3 (-CH(CH₃^ACH₃^B)), 22.9 (-CH(CH₃^ACH₃^B)), 17.3 (-CH₃^{aryl}), 13.8 (-CH₃^{alkyl}).

X-ray crystal structure analysis of **5a**: formula C₂₄H₃₁N₃, *M_r* = 361.52, light yellow crystal, 0.25 × 0.10 × 0.05 mm, *a* = 8.420(3) Å, *b* = 11.852(1) Å, *c* = 12.291(2) Å, α = 109.84(1)°, β = 108.27(2)°, γ = 90.96(2)°, *V* = 1085.1(4) Å³, ρ_{calcd} = 1.106 g cm⁻³, μ = 0.497 mm⁻¹, empirical absorption correction (0.886 ≤ *T* ≤ 0.976), *Z* = 2, triclinic, space group *P* $\bar{1}$ (No. 2), λ = 1.541 78 Å, *T* = 223 K, ω/2θ scans, 4738 reflections collected (±*h*, ±*k*, ±*l*), (sin θ)/λ = 0.62 Å⁻¹, 4424 independent (*R*_{int} = 0.063) and 2504 observed reflections (*I* ≥ 2σ(*I*)), 251 refined parameters, *R*1 = 0.056, *wR*2 = 0.162, maximum (minimum) residual electron density 0.22 (−0.21) e Å⁻³, hydrogen atoms calculated and refined as riding atoms.

Preparation of Ligand 5b. A sample of **3** (10.0 g, 31.0 mmol) in 150 mL of methanol was treated with 3-butenylamine (**4b**; 4.30 mL, 3.31 g, 46.5 mmol, 1.5 equiv) to yield a yellow solid (78%, 9.10 g, 24.2 mmol). Mp (DSC): 100 °C. MS-ESI (MeOH, ES⁺): *m/z* 398.3 ($[M + Na]^+$), 376.3 ($[M + H]^+$). Anal. Calcd for C₂₅H₃₃N₃ (375.55): C, 79.95; H, 8.86; N, 11.19. Found: C, 79.83; H, 8.73; N, 11.03. ¹H NMR (*d*₂-dichloromethane, 600 MHz, 298 K): δ(¹H) 8.35 (dd, ³*J* = 7.9 Hz, ⁴*J* = 1.0 Hz, 1H, 3-HPy), 8.20 (dd, ³*J* = 7.9 Hz, ⁴*J* = 1.0 Hz, 1H, 5-HPy), 7.83 (t, ³*J* = 7.9 Hz,

1H, 4-H^{py}), 7.16 (m, 2H, 3-H^{aryl}), 7.08 (m, 1H, 4-H^{aryl}), 5.99 (ddt, ³J = 17.2 Hz, ³J = 10.3 Hz, ³J = 6.8 Hz, 1H, =CH=), 5.15 (ddt, ³J = 17.2 Hz, ²J = 2.0 Hz, ⁴J = 1.6 Hz, 2H, =CH₂^Z), 5.05 (ddt, ³J = 10.3 Hz, ²J = 2.0 Hz, ⁴J = 1.2 Hz, 1H, =CH₂^E), 3.62 (d, ³J = 7.2 Hz, 1H, =NCH₂-), 2.75 (sept, ³J = 6.9 Hz, 2H, -CH(CH₃)₂), 2.53 (m, 2H, =NCH₂CH₂-), 2.41 (t, ⁵J = 0.7 Hz, 3H, -CH₃^{alkyl}), 2.24 (s, 3H, -CH₃^{aryl}), 1.15 (d, ³J = 6.9 Hz, 6H, -CH(CH₃^ACH₃^B)), 1.13 (d, ³J = 6.9 Hz, 6H, -CH(CH₃^ACH₃^B)). ¹³C{¹H} NMR (*d*₂-dichloromethane, 150 MHz, 298 K): δ(¹³C) 167.5 (N=C^{aryl}), 166.6 (N=C^{alkyl}), 156.9 (C-6^{py}), 155.1 (C-2^{py}), 147.0 (C-1^{aryl}), 137.6 (-CH=), 136.9 (C-4^{py}), 136.2 (C-2^{aryl}), 123.8 (C-4^{aryl}), 123.3 (C-3^{aryl}), 122.0 (C-5^{py}), 121.6 (C-3^{py}), 115.7 (=CH₂), 52.4 (=NCH₂-), 35.6 (=NCH₂CH₂-), 28.6 (CH(CH₃)₂), 23.3 (-CH(CH₃^ACH₃^B)), 22.9 (-CH(CH₃^ACH₃^B)), 17.3 (-CH₃^{aryl}), 13.8 (-CH₃^{alkyl}).

X-ray crystal structure analysis of **5b**: formula C₂₅H₃₃N₃, *M_r* = 375.54, light yellow crystal, 0.40 × 0.20 × 0.10 mm, *a* = 8.459(1) Å, *b* = 11.490(1) Å, *c* = 12.480(1) Å, α = 100.34(1)°, β = 107.97(1)°, γ = 95.02(1)°, *V* = 1121.8(2) Å³, ρ_{calcd} = 1.112 g cm⁻³, μ = 0.497 mm⁻¹, empirical absorption correction (0.826 ≤ *T* ≤ 0.952), *Z* = 2, triclinic, space group *P*1̄ (No. 2), λ = 1.541 78 Å, *T* = 223 K, ω and φ scans, 14 463 reflections collected (±*h*, ±*k*, ±*l*), (sin θ)/λ = 0.60 Å⁻¹, 3834 independent (*R*_{int} = 0.032) and 3499 observed reflections (*I* ≥ 2σ(*I*)), 259 refined parameters, *R*₁ = 0.051, w*R*₂ = 0.142, maximum (minimum) residual electron density 0.20 (-0.16) e Å⁻³, hydrogen atoms calculated and refined as riding atoms.

Preparation of Ligand 5c. A sample of **3** (2.40 g, 7.44 mmol) in 60 mL of methanol was treated with 4-pentenylamine (**4c**; 2.47 mL, 1.90 g, 22.3 mmol, 3 equiv) to yield a yellow solid (81%, 2.35 g, 6.03 mmol). Mp (DSC): 85 °C. MS-ESI (MeOH, ES⁺): *m/z* 412.3 ([M + Na]⁺), 390.3 ([M + H]⁺). Anal. Calcd for C₂₆H₃₅N₃ (389.58): C, 80.16; H, 9.06; N, 10.79. Found: C, 79.91; H, 9.02; N, 10.67. ¹H NMR (*d*₂-dichloromethane, 500 MHz, 298 K): δ(¹H) 8.36 (dd, ³J = 7.9 Hz, ⁴J = 1.0 Hz, 1H, 3-H^{py}), 8.22 (dd, ³J = 7.9 Hz, ⁴J = 1.0 Hz, 1H, 5-H^{py}), 7.84 (t, ³J = 7.9 Hz, 1H, 4-H^{py}), 7.17 (m, 2H, 3-H^{aryl}), 7.08 (m, 1H, 4-H^{aryl}), 5.93 (ddt, ³J = 17.2 Hz, ³J = 10.3 Hz, ³J = 6.7 Hz, 1H, =CH=), 5.08 (ddt, ³J = 17.2 Hz, ²J = 2.1 Hz, ⁴J = 1.6 Hz, 1H, =CH₂^Z), 5.00 (ddt, ³J = 10.3 Hz, ²J = 2.1 Hz, ⁴J = 1.2 Hz, 1H, =CH₂^E), 3.56 (t, ³J = 7.2 Hz, 2H, =NCH₂-), 2.78 (sept, ³J = 7.0 Hz, 2H, -CH(CH₃)₂), 2.41 (t, ⁵J = 0.8 Hz, 3H, -CH₃^{alkyl}), 2.25 (s, 3H, -CH₃^{aryl}), 2.24 (m, 2H, =NCH₂CH₂CH₂-), 1.88 (quint, ³J = 7.2 Hz, 2H, =NCH₂CH₂-), 1.16 (d, ³J = 7.0 Hz, 6H, -CH(CH₃^ACH₃^B)), 1.14 (d, ³J = 7.0 Hz, 6H, -CH(CH₃^ACH₃^B)). ¹³C{¹H} NMR (*d*₂-dichloromethane, 125 MHz, 298 K): δ(¹³C) 167.5 (N=C^{aryl}), 166.3 (N=C^{alkyl}), 157.1 (C-6^{py}), 155.2 (C-2^{py}), 147.0 (C-1^{aryl}), 139.2 (-CH=), 136.9 (C-4^{py}), 136.2 (C-2^{aryl}), 123.8 (C-4^{aryl}), 123.3 (C-3^{aryl}), 122.0 (C-5^{py}), 121.6 (C-3^{py}), 114.7 (=CH₂), 52.1 (=NCH₂-), 32.2 (=NCH₂CH₂CH₂-), 30.6 (=NCH₂CH₂-), 28.6 (-CH(CH₃)₂), 23.4 (-CH(CH₃^ACH₃^B)), 23.0 (-CH(CH₃^ACH₃^B)), 17.3 (-CH₃^{aryl}), 13.7 (-CH₃^{alkyl}).

X-ray crystal structure analysis of **5c**: formula C₂₆H₃₅N₃, *M_r* = 389.57, colorless crystal, 0.30 × 0.15 × 0.10 mm, *a* = 9.247(1) Å, *b* = 20.691(1) Å, *c* = 12.481(1) Å, β = 94.74(1)°, *V* = 2379.8(3) Å³, ρ_{calcd} = 1.087 g cm⁻³, μ = 0.484 mm⁻¹, empirical absorption correction (0.868 ≤ *T* ≤ 0.953), *Z* = 4, monoclinic, space group *P*2₁/*c* (No. 14), λ = 1.541 78 Å, *T* = 223 K, ω and φ scans, 16 747 reflections collected (±*h*, ±*k*, ±*l*), (sin θ)/λ = 0.60 Å⁻¹, 4225 independent (*R*_{int} = 0.045) and 3369 observed reflections (*I* ≥ 2σ(*I*)), 296 refined parameters, *R*₁ = 0.054, w*R*₂ = 0.151, group C26-C29 refined with split positions, maximum (minimum) residual electron density 0.37 (-0.22) e Å⁻³, hydrogen atoms calculated and refined as riding atoms.

Preparation of Ligand 5d. A sample of **3** (1.00 g, 3.10 mmol) in 60 mL of methanol was treated with 5-hexenylamine (**4d**; 1.70 mL, 1.23 g, 12.4 mmol, 4 equiv) to yield a deep yellow solid (60%, 0.75 g, 1.86 mmol). Mp (DSC): 60 °C. MS-ESI (MeOH, ES⁺):

m/z 426.3 ([M + Na]⁺), 404.3 ([M + H]⁺). Anal. Calcd for C₂₇H₃₇N₃ (403.60): C, 80.35; H, 9.24; N, 10.41. Found: C, 80.24; H, 9.19; N, 10.35. ¹H NMR (*d*₂-dichloromethane, 600 MHz, 298 K): δ(¹H) 8.37 (d, ³J = 7.6 Hz, 1H, 3-H^{py}), 8.22 (d, ³J = 7.6 Hz, 1H, 5-H^{py}), 7.84 (t, ³J = 7.6 Hz, 1H, 4-H^{py}), 7.18 (m, 2H, 3-H^{aryl}), 7.09 (m, 1H, 4-H^{aryl}), 5.90 (ddt, ³J = 17.3 Hz, ³J = 10.1 Hz, ³J = 6.8 Hz, 1H, =CH=), 5.06 (d, ³J = 17.3 Hz, 1H, =CH₂^Z), 4.98 (d, ³J = 10.1 Hz, 1H, =CH₂^E), 3.57 (t, ³J = 7.3 Hz, 2H, =NCH₂-), 2.77 (sept, ³J = 7.0 Hz, 2H, -CH(CH₃)₂), 2.43 (s, 3H, -CH₃^{alkyl}), 2.26 (s, 3H, -CH₃^{aryl}), 2.17 (q, ³J = 7.3 Hz, 2H, =NCH₂CH₂CH₂CH₂-), 1.80 (quint, ³J = 7.3 Hz, 2H, =NCH₂CH₂CH₂-), 1.59 (quint, ³J = 7.3 Hz, 2H, =NCH₂CH₂CH₂-), 1.17 (d, ³J = 7.0 Hz, 6H, -CH(CH₃^ACH₃^B)), 1.15 (d, ³J = 7.0 Hz, 6H, -CH(CH₃^ACH₃^B)). ¹³C{¹H} NMR (*d*₂-dichloromethane, 150 MHz, 298 K): δ(¹³C) 167.5 (N=C^{aryl}), 166.2 (N=C^{alkyl}), 157.1 (C-6^{py}), 155.2 (C-2^{py}), 147.0 (C-1^{aryl}), 139.5 (-CH=), 136.9 (C-4^{py}), 136.2 (C-2^{aryl}), 123.9 (C-4^{aryl}), 123.3 (C-3^{aryl}), 122.0 (C-5^{py}), 121.6 (C-3^{py}), 114.5 (=CH₂), 52.7 (=NCH₂-), 34.1 (=NCH₂CH₂CH₂CH₂-), 30.8 (=NCH₂CH₂-), 28.6 (-CH(CH₃)₂), 27.4 (=NCH₂CH₂CH₂-), 23.4 (-CH(CH₃^ACH₃^B)), 23.0 (-CH(CH₃^ACH₃^B)), 17.3 (-CH₃^{aryl}), 13.7 (-CH₃^{alkyl}).

Preparation of Ligand 6b. A sample of **3** (1.00 g, 3.10 mmol) in 60 mL of methanol was treated with *n*-butylamine (3.06 mL, 2.27 g, 31.0 mmol, 10 equiv) to yield a light yellow solid (90%, 1.05 g, 2.78 mmol). Mp (DSC): 93 °C. MS-ESI (MeOH, ES⁺): *m/z* 400.3 ([M + Na]⁺), 378.3 ([M + H]⁺). Anal. Calcd for C₂₅H₃₅N₃ (377.57): C, 79.53; H, 9.34; N, 11.13. Found: C, 79.34; H, 9.32; N, 10.94. ¹H NMR (*d*₂-dichloromethane, 600 MHz, 298 K): δ(¹H) 8.34 (d, ³J = 7.8 Hz, 1H, 3-H^{py}), 8.20 (d, ³J = 7.8 Hz, 1H, 5-H^{py}), 7.83 (t, ³J = 7.8 Hz, 1H, 4-H^{py}), 7.16 (m, 2H, 3-H^{aryl}), 7.08 (m, 1H, 4-H^{aryl}), 3.55 (t, ³J = 7.4 Hz, 2H, =NCH₂-), 2.75 (sept, ³J = 6.9 Hz, 2H, -CH(CH₃)₂), 2.41 (s, 3H, -CH₃^{alkyl}), 2.24 (s, 3H, -CH₃^{aryl}), 1.74 (quint, ³J = 7.4 Hz, 2H, =NCH₂CH₂-), 1.49 (sext, ³J = 7.4 Hz, 2H, =NCH₂CH₂CH₂-), 1.15 (d, ³J = 6.9 Hz, 6H, -CH(CH₃^ACH₃^B)), 1.13 (d, ³J = 6.9 Hz, 6H, -CH(CH₃^ACH₃^B)), 0.99 (t, ³J = 7.4 Hz, 3H, -CH₃). ¹³C{¹H} NMR (*d*₂-dichloromethane, 150 MHz, 298 K): δ(¹³C) 167.6 (N=C^{aryl}), 166.1 (N=C^{alkyl}), 157.1 (C-6^{py}), 155.1 (C-2^{py}), 147.0 (C-1^{aryl}), 136.9 (C-4^{py}), 136.2 (C-2^{aryl}), 123.8 (C-4^{aryl}), 123.3 (C-3^{aryl}), 122.0 (C-5^{py}), 121.5 (C-3^{py}), 52.6 (=NCH₂-), 33.5 (=NCH₂CH₂-), 28.6 (-CH(CH₃)₂), 23.3 (-CH(CH₃^ACH₃^B)), 22.9 (-CH(CH₃^ACH₃^B)), 21.2 (=NCH₂CH₂CH₂-), 17.3 (-CH₃^{aryl}), 14.2 (-CH₃), 13.6 (-CH₃^{alkyl}).

X-ray crystal structure analysis of **6b**: formula C₂₅H₃₅N₃, *M_r* = 377.56, colorless crystal, 0.40 × 0.30 × 0.30 mm, *a* = 12.387(1) Å, *b* = 16.007(1) Å, *c* = 12.911(1) Å, β = 115.16(1)°, *V* = 2317.1(3) Å³, ρ_{calcd} = 1.082 g cm⁻³, μ = 0.064 mm⁻¹, empirical absorption correction (0.975 ≤ *T* ≤ 0.981), *Z* = 4, monoclinic, space group *P*2₁/*n* (No. 14), λ = 0.710 73 Å, *T* = 198 K, ω and φ scans, 16 813 reflections collected (±*h*, ±*k*, ±*l*), (sin θ)/λ = 0.67 Å⁻¹, 5554 independent (*R*_{int} = 0.051) and 3258 observed reflections (*I* ≥ 2σ(*I*)), 260 refined parameters, *R*₁ = 0.065, w*R*₂ = 0.184, maximum (minimum) residual electron density 0.36 (-0.23) e Å⁻³, hydrogen atoms calculated and refined as riding atoms.

General Procedure for the Preparation of the Metal Complexes 7a-d, 8a-d, 9b, and 10b. A flame-dried Schlenk flask was charged under argon with the metal halide and *n*-butanol. To another Schlenk flask were added the corresponding Schiff base ligand (1.1 equiv) and *n*-butanol under inert conditions. Both Schlenk flasks were heated to 80 °C for 1 h, and then the ligand solution was transferred to the reaction vessel under argon, which contained the dissolved metal halide. The reaction mixture was heated further for 1 h and then stirred for 12 h at room temperature. Subsequently the volume of the solvent was reduced in vacuo. The precipitation was completed by addition of pentane (80 mL), and the solid was collected by filtration, washed with pentane until the

solvent was colorless, and dried in vacuo to give green solids in the case of the cobalt complexes **7a–d** and blue solids in the case of the iron complexes **8a–d**.

Preparation of Complex 7a. A sample of ligand **5a** (1.10 g, 3.05 mmol) was treated with cobalt(II) chloride (0.36 g, 2.77 mmol) in 40 mL of *n*-butanol to yield the green product (96%, 1.31 g, 2.67 mmol). Slow crystallization from a saturated dichloromethane solution gave single crystals of **7a** for the crystal structure analysis. Mp (DSC): 260 °C. MS-ESI (CH₃CN, ES⁺): *m/z* 455.2 ([M – Cl]⁺). Anal. Calcd for C₂₄H₃₁Cl₂CoN₃ (491.36): C, 58.66; H, 6.36; N, 8.55. Found: C, 58.67; H, 6.34; N, 8.25. IR (ATR): $\tilde{\nu}$ (cm⁻¹) 2962, 2925, 2868, 1623, 1581, 1463, 1379, 1370, 1319, 1268, 1246, 1203, 1059, 1027, 981, 912, 773, 744, 703, 607, 546.

X-ray crystal structure analysis of **7a**: formula C₂₄H₃₁Cl₂CoN₃, *M_r* = 491.35, yellow crystal, 0.40 × 0.20 × 0.05 mm, *a* = 17.433(1) Å, *b* = 9.802(1) Å, *c* = 15.579(1) Å, β = 115.26(1)°, *V* = 2407.6(3) Å³, ρ_{calcd} = 1.356 g cm⁻³, μ = 0.950 mm⁻¹, empirical absorption correction (0.702 ≤ *T* ≤ 0.954), *Z* = 4, monoclinic, space group *P*2₁/*c* (No. 14), λ = 0.710 73 Å, *T* = 198 K, ω and φ scans, 14 065 reflections collected ($\pm h, \pm k, \pm l$), (sin θ)/ λ = 0.67 Å⁻¹, 5827 independent (*R*_{int} = 0.057) and 4689 observed reflections (*I* ≥ 2σ(*I*)), 278 refined parameters, *R*1 = 0.082, *wR*2 = 0.216, maximum (minimum) residual electron density 3.22 (–0.86) e Å⁻³ close to Co and Cl, hydrogen atoms calculated and refined as riding atoms, due to crystal twinning the analysis is of poor quality.

Preparation of Complex 7b. A sample of ligand **5b** (337 mg, 0.90 mmol) was treated with cobalt(II) chloride (106 mg, 0.82 mmol) in 20 mL of *n*-butanol to yield the green product (99%, 409 mg, 0.81 mmol). Slow crystallization from a saturated dichloromethane solution gave single crystals of **7b** for the crystal structure analysis. Mp (DSC): 288 °C. MS-ESI (CH₃CN, ES⁺): *m/z* 469.4 ([M – Cl]⁺). Anal. Calcd for C₂₅H₃₃Cl₂CoN₃ (505.39): C, 59.41; H, 6.58; N, 8.31. Found: C, 59.27; H, 6.65; N, 8.13. IR (ATR): $\tilde{\nu}$ (cm⁻¹) 2963, 2923, 2871, 1587, 1467, 1370, 1264, 1203, 1105, 1010, 918, 810, 773, 741, 634, 545.

X-ray crystal structure analysis of **7b**: formula C₂₅H₃₃Cl₂CoN₃, *M_r* = 505.37, yellow crystal, 0.35 × 0.10 × 0.03 mm, *a* = 17.509(1) Å, *b* = 9.837(1) Å, *c* = 15.598(1) Å, β = 114.40(1)°, *V* = 2446.6(3) Å³, ρ_{calcd} = 1.372 g cm⁻³, μ = 0.937 mm⁻¹, empirical absorption correction (0.735 ≤ *T* ≤ 0.972), *Z* = 4, monoclinic, space group *P*2₁/*c* (No. 14), λ = 0.710 73 Å, *T* = 198 K, ω and φ scans, 14 485 reflections collected ($\pm h, \pm k, \pm l$), (sin θ)/ λ = 0.67 Å⁻¹, 5853 independent (*R*_{int} = 0.048) and 4213 observed reflections (*I* ≥ 2σ(*I*)), 286 refined parameters, *R*1 = 0.042, *wR*2 = 0.080, maximum (minimum) residual electron density 0.33 (–0.41) e Å⁻³, hydrogen atoms calculated and refined as riding atoms.

Preparation of Complex 7c. A sample of ligand **5c** (300 mg, 0.77 mmol) was treated with cobalt(II) chloride (90.9 mg, 0.70 mmol) in 20 mL of *n*-butanol to yield the green product (96%, 350 mg, 0.67 mmol). Slow crystallization from a saturated dichloromethane solution gave single crystals of **7c** for the crystal structure analysis. Mp (DSC): 308 °C. Anal. Calcd for C₂₆H₃₅Cl₂CoN₃ (519.42): C, 60.12; H, 6.79; N, 8.09; Found: C, 60.03; H, 6.81; N, 7.96. IR (ATR): $\tilde{\nu}$ (cm⁻¹) 2961, 2928, 2866, 1583, 1461, 1441, 1364, 1259, 1203, 1103, 1057, 1203, 1103, 1057, 1025, 996, 925, 817, 773, 745, 653.

X-ray crystal structure analysis of **7c**: formula C₂₆H₃₅Cl₂CoN₃, *M_r* = 519.40, yellow crystal, 0.50 × 0.40 × 0.03 mm, *a* = 9.451(1) Å, *b* = 13.486(1) Å, *c* = 10.434(1) Å, β = 95.63(1)°, *V* = 1323.5(2) Å³, ρ_{calcd} = 1.303 g cm⁻³, μ = 0.868 mm⁻¹, empirical absorption correction (0.671 ≤ *T* ≤ 0.974), *Z* = 2, monoclinic, space group *P*2₁ (No. 4), λ = 0.710 73 Å, *T* = 198 K, ω and φ scans, 8798 reflections collected ($\pm h, \pm k, \pm l$), (sin θ)/ λ = 0.67 Å⁻¹, 5403 independent (*R*_{int} = 0.040) and 4798 observed reflections (*I* ≥ 2σ(*I*)), 295 refined parameters, *R*1 = 0.039, *wR*2 = 0.096, Flack parameter 0.00(2), maximum (minimum) residual electron density 0.87 (–0.34) e Å⁻³, hydrogen atoms calculated and refined as riding atoms.

Preparation of Complex 7d. A sample of ligand **5d** (500 mg, 1.24 mmol) was treated with cobalt(II) chloride (160 mg, 1.23 mmol) in 40 mL of *n*-butanol to yield the green product (82%, 538 mg, 1.01 mmol). Slow crystallization from a saturated dichloromethane solution gave single crystals of **7d** for the crystal structure analysis. Mp (DSC): 301 °C. MS-ESI (CH₃CN, ES⁺): *m/z* 497.5 ([M – Cl]⁺). Anal. Calcd for C₂₇H₃₇Cl₂CoN₃ (533.44): C, 60.79; H, 6.99; N, 7.88. Found: C, 60.58; H, 7.00; N, 7.77. IR (ATR): $\tilde{\nu}$ (cm⁻¹) 2962, 2929, 2867, 1624, 1582, 1462, 1441, 1364, 1318, 1262, 1203, 1179, 1102, 996, 908, 816, 806, 773, 744, 696, 641.

X-ray crystal structure analysis of **7d**: formula C₂₇H₃₇Cl₂CoN₃, *M_r* = 533.43, yellow crystal, 0.45 × 0.10 × 0.03 mm, *a* = 9.5883(3) Å, *b* = 12.9838(2) Å, *c* = 10.8393(4) Å, β = 92.006(2)°, *V* = 1348.59(7) Å³, ρ_{calcd} = 1.314 g cm⁻³, μ = 0.854 mm⁻¹, empirical absorption correction (0.700 ≤ *T* ≤ 0.975), *Z* = 2, monoclinic, space group *P*2₁ (No. 4), λ = 0.710 73 Å, *T* = 198 K, ω and φ scans, 9205 reflections collected ($\pm h, \pm k, \pm l$), (sin θ)/ λ = 0.66 Å⁻¹, 5774 independent (*R*_{int} = 0.057) and 4552 observed reflections (*I* ≥ 2σ(*I*)), 323 refined parameters, *R*1 = 0.051, *wR*2 = 0.103, Flack parameter –0.02(2), group *C*29 to *C*30 refined with split positions, maximum (minimum) residual electron density 0.36 (–0.51) e Å⁻³, hydrogen atoms calculated and refined as riding atoms.

Preparation of Complex 8a. A sample of ligand **5a** (1.07 g, 2.95 mmol) was treated with iron(II) chloride (340 mg, 2.68 mmol) in 75 mL of *n*-butanol to yield the blue product (98%, 1.28 g, 2.62 mmol). Mp (DSC): 267 °C. MS-ESI (CH₃CN, ES⁺): *m/z* 511.2 ([M + Na]⁺), 452.2 ([M – Cl]⁺). Anal. Calcd for C₂₄H₃₁Cl₂FeN₃ (488.27): C, 60.79; H, 6.99; N, 7.88. Found: C, 60.58; H, 7.00; N, 7.77. IR (ATR): $\tilde{\nu}$ (cm⁻¹) 2963, 2926, 2868, 1581, 1461, 1444, 1370, 1323, 1272, 1247, 1203, 1179, 1104, 1059, 981, 912, 812, 773, 740.

Preparation of Complex 8b. A sample of ligand **5b** (250 mg, 0.67 mmol) was treated with iron(II) chloride (77.3 mg, 0.61 mmol) in 40 mL of *n*-butanol to yield the blue product (97%, 295 mg, 0.59 mmol). Mp (DSC): 292 °C. MS-ESI (CH₃CN, ES⁺): *m/z* 466.4 ([M – Cl]⁺). Anal. Calcd for C₂₅H₃₃Cl₂FeN₃ (502.30): C, 59.78; H, 6.62; N, 8.37. Found: C, 59.74; H, 6.65; N, 8.25. IR (ATR): $\tilde{\nu}$ (cm⁻¹) 2962, 2923, 2870, 1585, 1466, 1445, 1370, 1329, 1268, 1202, 1179, 1105, 1008, 918, 810, 773, 738, 673.

X-ray crystal structure analysis of **8b**: formula C₂₅H₃₃Cl₂FeN₃, *M_r* = 502.29, blue crystal, 0.30 × 0.15 × 0.02 mm, *a* = 17.316(5) Å, *b* = 9.809(4) Å, *c* = 15.391(3) Å, β = 114.315(9)°, *V* = 2382.3(13) Å³, ρ_{calcd} = 1.400 g cm⁻³, μ = 0.875 mm⁻¹, empirical absorption correction (0.779 ≤ *T* ≤ 0.983), *Z* = 4, monoclinic, space group *P*2₁/*c* (No. 14), λ = 0.710 73 Å, *T* = 198 K, ω and φ scans, 6713 reflections collected ($\pm h, \pm k, \pm l$), (sin θ)/ λ = 0.60 Å⁻¹, 3924 independent (*R*_{int} = 0.073) and 2351 observed reflections (*I* ≥ 2σ(*I*)), 286 refined parameters, *R*1 = 0.090, *wR*2 = 0.250, maximum (minimum) residual electron density 0.53 (–0.89) e Å⁻³, hydrogen atoms calculated and refined as riding atoms, due to crystal quality the analysis is of poor quality.

Preparation of Complex 8c. A sample of ligand **5c** (500 mg, 1.28 mmol) was treated with iron(II) chloride (148 mg, 1.17 mmol) in 40 mL of *n*-butanol to yield the blue product (83%, 500 mg, 0.97 mmol). Crystals suitable for X-ray diffraction were obtained from a warm concentrated solution of **8c** in tetrahydrofuran by slowly cooling to room temperature. Mp (DSC): 299 °C. MS-ESI (CH₃CN, ES⁺): *m/z* 538.0 ([M + Na]⁺), 480.1 ([M – Cl]⁺). Anal. Calcd for C₂₆H₃₅Cl₂FeN₃ (516.33): C, 60.48; H, 6.83; N, 8.14. Found: C, 59.79; H, 6.89; N, 8.01. IR (ATR): $\tilde{\nu}$ (cm⁻¹) 2961, 2927, 2870, 1580, 1442, 1365, 1327, 1265, 1201, 1177, 1104, 1056, 996, 924, 804, 773, 741, 698, 656.

X-ray crystal structure analysis of **8c**: formula C₂₆H₃₅Cl₂FeN₃, *M_r* = 516.32, blue crystal, 0.30 × 0.15 × 0.05 mm, *a* = 9.4994(2) Å, *b* = 13.5202(4) Å, *c* = 10.4090(3) Å, β = 95.779(1)°, *V* =

1330.07(6) Å³, $\rho_{\text{calcd}} = 1.289 \text{ g cm}^{-3}$, $\mu = 0.786 \text{ mm}^{-1}$, empirical absorption correction (0.798 $\leq T \leq$ 0.962), $Z = 2$, monoclinic, space group $P2_1$ (No. 4), $\lambda = 0.71073 \text{ \AA}$, $T = 198 \text{ K}$, ω and φ scans, 9064 reflections collected ($\pm h, \pm k, \pm l$), $(\sin \theta)/\lambda = 0.60 \text{ \AA}^{-1}$, 4230 independent ($R_{\text{int}} = 0.054$) and 3447 observed reflections ($I \geq 2\sigma(I)$), 295 refined parameters, $R1 = 0.066$, $wR2 = 0.177$, Flack parameter $-0.01(3)$, maximum (minimum) residual electron density $0.92 (-0.68) \text{ e \AA}^{-3}$, hydrogen atoms calculated and refined as riding atoms.

Preparation of Complex 8d. A sample of ligand **5d** (500 mg, 1.24 mmol) was treated with iron(II) chloride (156 mg, 1.23 mmol) in 40 mL of *n*-butanol to yield the blue product (60%, 393 mg, 0.74 mmol). Mp (DSC): 295 °C. MS-ESI (CH₃CN, ES⁺): m/z 494.5 ([M - Cl]⁺). Anal. Calcd for C₂₇H₃₇Cl₂FeN₃ (530.35): C, 61.15; H, 7.03; N, 7.92. Found: C, 61.07; H, 7.06; N, 7.87. IR (ATR): $\tilde{\nu}$ (cm⁻¹) 2963, 2927, 2872, 1639, 1588, 1463, 1443, 1368, 1268, 1255, 1212, 1109, 1058, 1021, 985, 904, 817, 800, 770, 745, 698, 622.

Preparation of Complex 9b. A sample of ligand **6b** (500 mg, 1.32 mmol) was treated with cobalt(II) chloride (163 mg, 1.26 mmol) in 40 mL of *n*-butanol to yield the green product (99%, 630 mg, 1.24 mmol). Mp (DSC): 308 °C. MS-ESI (CH₃CN, ES⁺): m/z 471.1 ([M - Cl]⁺). Anal. Calcd for C₂₅H₃₅Cl₂CoN₃ (507.40): C, 59.18; H, 6.95; N, 8.28. Found: C, 58.62; H, 7.04; N, 8.25. IR (ATR): $\tilde{\nu}$ (cm⁻¹) 2963, 2926, 2870, 1583, 1462, 1371, 1263, 1203, 1179, 1104, 1059, 1027, 939, 811, 775, 743, 696, 632.

Preparation of Complex 10b. A sample of ligand **6b** (500 mg, 1.32 mmol) was treated with iron(II) chloride (157 mg, 1.24 mmol) in 40 mL of *n*-butanol to yield the blue product (99%, 625 mg, 1.24 mmol). Mp (DSC): 307 °C. MS-ESI (CH₃CN, ES⁺): m/z 468.3 ([M - Cl]⁺). Anal. Calcd for C₂₅H₃₅Cl₂FeN₃ (504.32): C, 59.54; H, 7.00; N, 8.33. Found: C, 58.96; H, 6.99; N, 8.21. IR (ATR): $\tilde{\nu}$ (cm⁻¹) 2962, 2927, 2870, 1582, 1460, 1444, 1371, 1326, 1266, 1202, 1179, 1104, 1058, 1024, 939, 812, 772, 741, 699.

Preparation of Complex 11a. In a flame-dried Schlenk flask the [bis(imino)pyridine]CoCl₂ complex **7a** (200 mg, 0.41 mmol) and solid methyllithium (26.8 mg, 1.22 mmol, 3 equiv) were mixed with 20 mL of precooled diethyl ether at $-78 \text{ }^\circ\text{C}$. The mixture was then slowly warmed to $10 \text{ }^\circ\text{C}$ within 20 h with stirring. The solution was filtered under argon through Celite, and the separated lithium chloride was not washed further; instead, the solvent was rapidly removed in vacuo to yield the purple product **11a** (89%, 159 mg, 0.36 mmol). The product is stable for some weeks on storage in a glovebox. Crystals suitable for X-ray diffraction were obtained during the preparation in diethyl ether at $10 \text{ }^\circ\text{C}$. Mp (DSC): $149 \text{ }^\circ\text{C}$. Anal. Calcd for C₂₅H₃₄CoN₃ (435.49): C, 68.95; H, 7.87; N, 9.65. Found: C, 68.44; H, 7.93; N, 9.29. ¹H NMR (d_8 -toluene, 400 MHz, 298 K): δ (¹H) 10.10 (t, ³J = 7.5 Hz, 1H, 4-H^{py}), 7.68 (d, ³J = 7.5 Hz, 1H, 3-H^{py}), 7.53 (d, ³J = 7.5 Hz, 1H, 5-H^{py}), 7.49 (m, 1H, 4-H^{aryl}), 7.39 (m, 2H, 3-H^{aryl}), 6.40 (m, 1H, =CH=), 5.60 (br, 2H, =NCH₂-), 5.16 (d, ³J = 17.4 Hz, 1H, =CH₂^z), 4.96 (d, ³J = 10.8 Hz, 1H, =CH₂^f), 3.08 (sept, ³J = 6.7 Hz, 2H, -CH(CH₃)₂), 1.12 (d, ³J = 6.7 Hz, 6H, -CH(CH₃^ACH₃^B)), 0.61 (d, ³J = 6.7 Hz, 6H, -CH(CH₃^ACH₃^B)), 0.54 (s, 3H, Co-CH₃), -0.64 (s, 3H, -CH₃^{alkyl}), -1.51 (s, 3H, -CH₃^{aryl}). ¹³C{¹H} NMR (d_8 -toluene, 100 MHz, 298 K): δ 167.4 (N=C^{aryl}), 163.7 (N=C^{aryl}), 157.4 (C-6^{py}), 155.9 (C-2^{py}), 155.3 (C-1^{aryl}), 137.5 (C-2^{aryl}), 132.6 (-CH=), 126.5 (C-4^{aryl}), 123.9 (C-3^{aryl}), 122.6 (C-5^{py}), 121.9 (C-3^{py}), 116.6 (C-4^{py}), 115.4 (=CH₂), 61.3 (=NCH₂-), 28.5

(-CH(CH₃)₂), 25.5 (-CH₃^{aryl}), 23.9 (-CH(CH₃^ACH₃^B)), 23.4 (-CH(CH₃^ACH₃^B)), 22.0 (-CH₃^{alkyl}), n.o. (Co-CH₃).

X-ray crystal structure analysis of **11a**: formula C₂₅H₃₄CoN₃, $M_r = 435.48$, black crystal, $0.30 \times 0.10 \times 0.07 \text{ mm}$, $a = 12.706(1) \text{ \AA}$, $b = 11.551(1) \text{ \AA}$, $c = 15.914(1) \text{ \AA}$, $\beta = 98.78(1)^\circ$, $V = 2308.3(3) \text{ \AA}^3$, $\rho_{\text{calcd}} = 1.253 \text{ g cm}^{-3}$, $\mu = 0.759 \text{ mm}^{-1}$, empirical absorption correction (0.804 $\leq T \leq$ 0.949), $Z = 4$, monoclinic, space group $P2_1/c$ (No. 14), $\lambda = 0.71073 \text{ \AA}$, $T = 198 \text{ K}$, ω and φ scans, 19 588 reflections collected ($\pm h, \pm k, \pm l$), $(\sin \theta)/\lambda = 0.66 \text{ \AA}^{-1}$, 5499 independent ($R_{\text{int}} = 0.070$) and 3818 observed reflections ($I \geq 2\sigma(I)$), 269 refined parameters, $R1 = 0.046$, $wR2 = 0.106$, maximum (minimum) residual electron density $0.25 (-0.25) \text{ e \AA}^{-3}$, hydrogen atoms calculated and refined as riding atoms.

Catalytic Ethylene Polymerization. A 1 L Büchi glass autoclave with a catalyst reservoir and stirrer was evacuated and filled with argon three times before it was charged with 200 mL of toluene and 6.8 mL of 10% methylalumoxane in toluene. A precise amount of respective complex (0.05 mmol) was dissolved in 10 mL of toluene and then loaded into the catalyst reservoir. The stirrer was started (600 rpm), and the autoclave was thermostated at room temperature while the solution was saturated with ethylene at 2 bar, which was controlled by bpc 1202 (Büchi pressflow gas controller with program "bls2"). After the solution was saturated with ethylene (the line of consumption volume went flat), the catalyst solution in the reservoir was introduced directly into the autoclave. In the case of preactivation of the metal, 200 mL of toluene and 5 mL of 10% methylalumoxane in toluene was added to the Büchi autoclave and 1.8 mL was added to the catalyst solution before it was loaded into the catalyst reservoir. The polymerization reaction was stopped by terminating the transfer of ethylene with the bpc controller and quenching with 10 mL of aqueous HCl in methanol (1/1 v/v). The precipitated polyethylene was collected by filtration, washed subsequently with HCl, water, and acetone, and dried at $80 \text{ }^\circ\text{C}$ under vacuum overnight to constant weight. The polymer was characterized by DSC and ¹³C NMR. The obtained polymer is linear polyethylene. The oligomers were extracted from the water phase with diethyl ether, and the resulting organic solvent was removed in vacuo. The oligomers were characterized by GPC and ¹H NMR.

Ethene Polymerization for ESI-MS Mechanistic Studies. Under an inert atmosphere the respective complex (0.05 mmol) was reacted with 8 mL of 10% methylalumoxane in toluene in 30 mL of tetrahydrofuran in a 100 mL Schlenk flask. The flask was evacuated and purged with ethene (2 bar) at room temperature. The reaction mixture was stirred under a constant pressure of 1 bar of ethene for 0.5 h at room temperature. Then the ethene pressure was released, and the reaction was quenched with 2 mL of methanol. A sample from the supernatant was analyzed by mass spectrometry with a nano spray inlet.

Acknowledgment. Financial support from the Fonds der Chemischen Industrie and the Deutsche Forschungsgemeinschaft are gratefully acknowledged. We thank the BASF for a gift of solvents.

Supporting Information Available: Text, figures, and tables giving further experimental and spectroscopic details and CIF files giving crystallographic data. This material is available free of charge via the Internet at <http://pubs.acs.org>.

OM800726Y